

Cerebral serotonin transporter measurements with [¹¹C]DASB: A review on acquisition and preprocessing across 21 PET centres

Martin Nørgaard^{1,2}, Melanie Ganz^{1,3}, Claus Svarer¹, Ling Feng¹, Masanori Ichise⁴, Rupert Lanzenberger⁵, Mark Lubberink⁶, Ramin V Parsey⁷, Marios Politis⁸, Eugenii A Rabiner^{9,10}, Mark Slifstein⁷, Vesna Sossi¹¹, Tetsuya Suhara⁴, Peter S Talbot¹², Federico Turkheimer¹³, Stephen C Strother¹⁴ and Gitte M Knudsen^{1,2}

Abstract

Positron Emission Tomography (PET) imaging has become a prominent tool to capture the spatiotemporal distribution of neurotransmitters and receptors in the brain. The outcome of a PET study can, however, potentially be obscured by suboptimal and/or inconsistent choices made in complex processing pipelines required to reach a quantitative estimate of radioligand binding. Variations in subject selection, experimental design, data acquisition, preprocessing, and statistical analysis may lead to different outcomes and neurobiological interpretations. We here review the approaches used in 105 original research articles published by 21 different PET centres, using the tracer [¹¹C]DASB for quantification of cerebral serotonin transporter binding, as an exemplary case. We highlight and quantify the impact of the remarkable variety of ways in which researchers are currently conducting their studies, while implicitly expecting generalizable results across research groups. Our review provides evidence that the foundation for a given choice of a preprocessing pipeline seems to be an overlooked aspect in modern PET neuroscience. Furthermore, we believe that a thorough testing of pipeline performance is necessary to produce reproducible research outcomes, avoiding biased results and allowing for better understanding of human brain function.

Keywords

Positron Emission Tomography, preprocessing, kinetic modeling, [¹¹C]DASB, data sharing

Received 18 October 2017; Revised 7 March 2018; Accepted 7 March 2018

¹Neurobiology Research Unit, Copenhagen University Hospital, Rigshospitalet, Copenhagen, Denmark

²Faculty of Health Sciences, University of Copenhagen, Copenhagen, Denmark

³Department of Computer Science, University of Copenhagen, Copenhagen, Denmark

⁴Department of Functional Brain Imaging Research, National Institute of Radiological Sciences, National Institutes for Quantum and Radiological Science and Technology, Chiba, Japan

⁵Department of Psychiatry and Psychotherapy, Medical University of Vienna, Vienna, Austria

⁶Department of Nuclear Medicine and Positron Emission Tomography, Uppsala University, Uppsala, Sweden

⁷Department of Psychiatry, School of Medicine, Stony Brook University, Stony Brook, NY, USA

⁸Neurodegeneration Imaging Group, Institute of Psychiatry, Psychology and Neuroscience (IoPPN), King's College London, London, UK

⁹Imanova Limited, London, UK

¹⁰Centre for Neuroimaging Sciences, Institute of Psychiatry, Psychology and Neuroscience, King's College London, London, UK

¹¹Department of Physics and Astronomy, University of British Columbia, Vancouver, BC, Canada

¹²Division of Neuroscience and Experimental Psychology, School of Biological Sciences, Faculty of Biology, Medicine and Health, University of Manchester, Manchester Academic Health Science Centre, Manchester, UK

¹³Department of Neuroimaging, King's College London, London, UK

¹⁴Rotman Research Institute at Baycrest, University of Toronto, Toronto, Canada

Corresponding author:

Gitte M Knudsen, Neurobiology Research Unit, Section 6931, Rigshospitalet 9, Blegdamsvej DK-2100, Copenhagen.
Email: gmk@nru.dk

Introduction

Positron Emission Tomography (PET) imaging with selective radiotracers has been extensively used as a tool for novel neuroscience research. PET neuroimaging often utilizes complex workflows, with multiple stages ranging from subject selection, experimental design, data acquisition, preprocessing, statistical analysis to the final neurobiological interpretation.

However, while most published articles utilizing molecular neuroimaging have mainly focused on extracting neuroscientifically relevant results, no articles have, to our knowledge, investigated the extent to which these findings may be significantly influenced by different sets of preprocessing steps (“preprocessing pipeline/stage”) applied while analyzing the data. A preprocessing pipeline in neuroimaging commonly refers to a set of steps used to denoise and remove artifacts in the data for subsequent statistical analysis (e.g. motion correction and outlier detection), thereby improving the overall quality of the data. However, choices made at any stage of a neuroimaging workflow may significantly affect the chosen steps in the preprocessing pipeline, limiting the generalizability of any preprocessing pipeline studied in isolation from a fixed neuroimaging workflow. For example, medical conditions preventing patients from staying still in the scanner (e.g. Parkinson’s Disease) may require more extensive correction of head movements in the preprocessing stage compared to healthy subjects.

Notably, to date, preprocessing developments in the PET neuroimaging community have often been

focusing on an even more limited point of view than examining the overall preprocessing pipeline in isolation. The optimization of preprocessing steps typically entails only limited test data, and is often performed with the aim of optimizing only a single preprocessing step (e.g. kinetic modeling) without explicitly attempting to address potential interactions with other preprocessing steps, or with other stages of a given workflow. Examples of such potential confounds include: subject selection (e.g. of healthy versus diseased cohorts), differences in scanner resolution, duration of a scanning session, dynamic framing, injected dose/injected mass (data acquisition), differences in image reconstruction, motion correction, different kinetic modeling approaches used to estimate the availability of receptors/transporters (preprocessing), and different statistical model choices used to test for group or longitudinal differences (statistical analysis).

We here review and quantify the impact of the various data acquisition and preprocessing pipeline choices used to quantify the same biological target, using the serotonin transporter and the radioligand [¹¹C]DASB as exemplary case. We chose to specifically focus on the serotonin transporter using [¹¹C]DASB, because this is a well established radioligand in the field and has been used extensively to study various aspects of brain function ranging from schizophrenia to epilepsy (Figure 1).

Since [¹¹C]DASB was first described in 2000¹ through the end of March 2017, nearly 170 [¹¹C]DASB PET papers have been published, and this

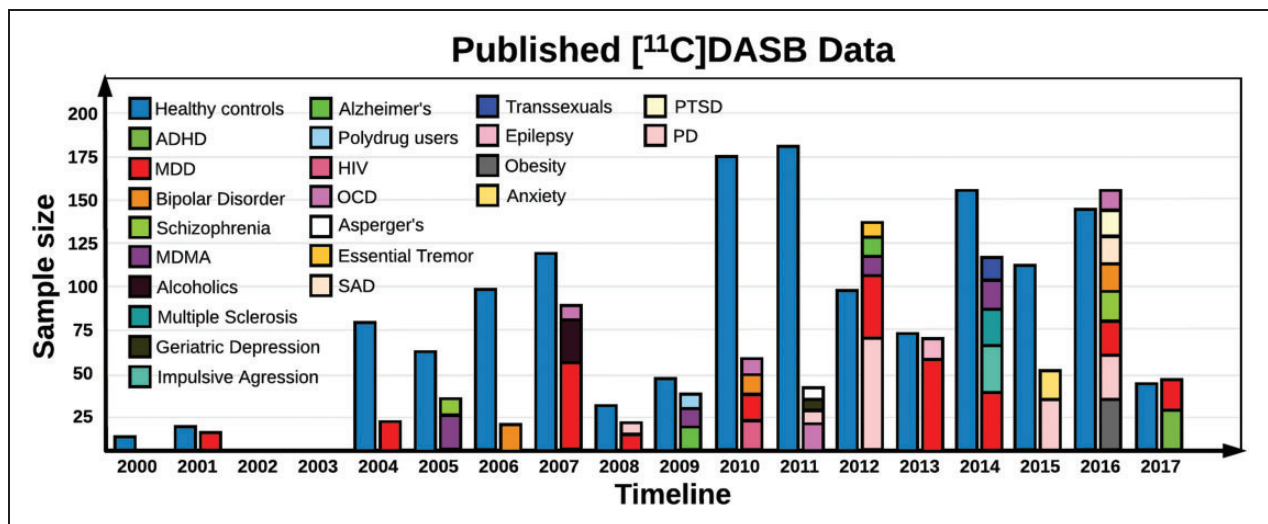


Figure 1. Timeline of number of patient and healthy controls in the 105 published [¹¹C]DASB studies. The colors indicate either healthy controls, or a specific disorder as a function of time and sample size. ADHD: attention-deficit/hyperactive disorder; MDD: major depressive disorder; MDMA: ecstasy; HIV: human immunodeficiency virus; OCD: obsessive compulsive disorder; SAD: seasonal affective disorder; PTSD: post-traumatic stress syndrome; PD: Parkinson’s disease.

number is growing by one to two articles per month. We systematically searched PubMed for studies using “[¹¹C]DASB and PET” in the time period between September 2000 to March 2017, and found a total of 169 publications. Non-human studies (N=49), reviews (N=4), and methodological papers (N=12) were excluded due to substantial differences in acquisition and preprocessing, leaving 104 publications eligible for scrutiny. One paper not identified by the search,² was subsequently added, summing up to a total of 105 original research articles. We catalogued the different sample sizes and patient cohorts investigated in the published [¹¹C]DASB studies, the various data acquisition techniques used, and the preprocessing steps applied to the data. We systematically outline and quantify the impact of the remarkable variety of ways in which researchers are currently performing these studies, while implicitly expecting generalizable results across research groups. Although this review specifically focuses on the radioligand [¹¹C]DASB, the underlying considerations apply to any given PET or SPECT radiotracer, as optimal neuroimaging workflows are highly dependent on the inherent characteristics of the radioligand of interest.

Data acquisition workflow and outcome

In order to investigate the variability in data acquisition and preprocessing, we provide an overview of the different acquisition and preprocessing choices that have been made in previous studies. We also examine how differences in reported findings might be influenced by differences in methodologies. For this purpose, we extract the [¹¹C]DASB PET binding potentials (BP_{ND}) in striatum and anterior cingulate cortex (ACC) as well as other relevant information from 90 studies with healthy controls encompassing a total of 1856 healthy controls. We chose to examine the healthy controls only because they serve as null data, achieved with different experimental designs. The available BP_{ND}'s and standard deviations from the published studies were used as the dependent variable in separate linear models, correcting for the number of healthy controls included in the study, age, age standard deviation, choice of MRI hardware, choice of PET hardware, number of frames, injected dose, motion correction, choice of volumes-of-interest (VOI), and choice of kinetic modeling (Table S1). All covariates were standardized columnwise to have mean 0 and standard deviation 1. To limit the degrees of freedom, we did not specify any interactions in the linear model, despite their obvious existence (e.g. PET scanner × injected dose).

The omission of potential interactions is a limitation of the current analysis, but is driven by limited data.

Development of [¹¹C]DASB in PET neuroimaging and subject selection

N,N-dimethyl-2-(2-amino-4-cyanophenylthio)benzylamine, or more commonly referred to as DASB, was developed by Wilson et al. at the Center for Addiction and Mental Health, Toronto Canada, and their first-in-human study was published in 2000.^{1,3}

Their preliminary analyses indicated that DASB radiolabeled with carbon-11 effectively penetrated the blood–brain barrier, and displayed retention characteristics in accordance with the known anatomical distribution of cerebral serotonin reuptake sites. In any aspect, [¹¹C]DASB turned out to be a highly suitable radiotracer to map the serotonin transporter using dynamic 4D PET imaging.

Since 2000, [¹¹C]DASB has been used extensively, so far by 21 PET centres, investigating various aspects of brain function. In Figure 1, we provide a timeline of the number of healthy controls and patient cohorts that have been investigated and published using [¹¹C]DASB. Whenever possible, we have attempted to correct the data in Figure 1 for duplicates, to encounter only the net number of included healthy volunteers from the [¹¹C]DASB PET studies.

Our analysis of the reported values from the literature suggests no statistical evidence for an impact of the number of subjects included in the study on BP_{ND} or between-subject variation.

We found a trend for an association between age and between-subject variation of ACC BP_{ND} ($P=0.075$), suggesting that between-subject ACC BP_{ND} is more variable in elderly than in young controls. While this may be caused by cortical atrophy or other age-related disorders, it warrants further examination of how the impact of acquisition and preprocessing choices may vary as a function of age.

PET scanners and reconstructions

We found that in the 21 centres, 9 different scanners have been used (Figure 2). The first paper published by Houle et al.³ (Center for Addiction and Mental Health, Toronto, Canada) presented data acquired with a Scanditronix/GEMS PC2048-15B 2D brain PET scanner, a state-of-the-art scanner from the late 80s. The data were attenuation corrected and reconstructed using filtered back-projection (FBP). The performance of the Scanditronix/GEMS PC2048-15B scanner was evaluated in 1989 by Holte et al.,⁴ reporting the in-plane axial full-width half maximum (FWHM) to be 5.9 mm for direct planes, and 5 mm for cross planes in the central area of the field-of-view (FOV). In addition, with a coincidence timing window of 12.5 ns and a lower energy threshold of 300 keV,

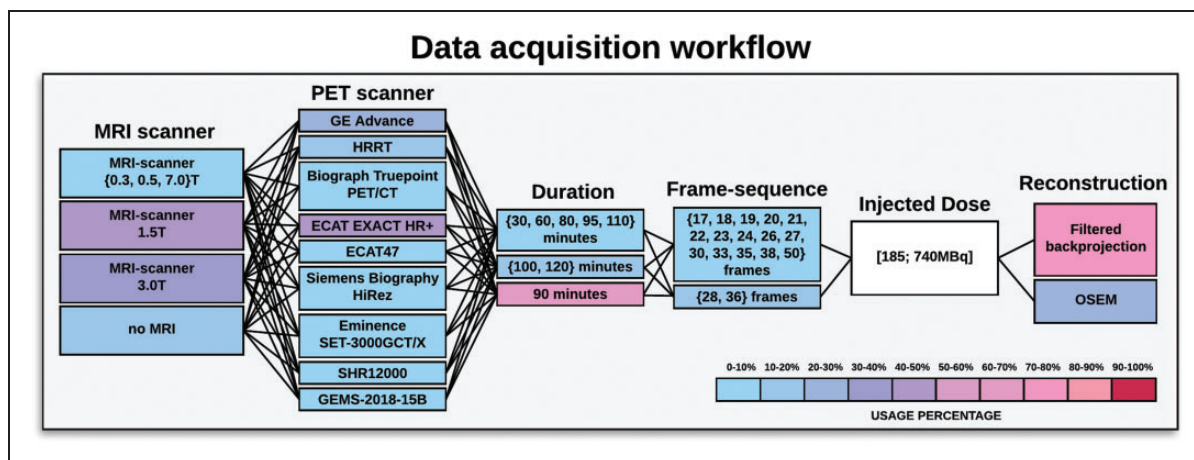


Figure 2. Schematic overview of the different data acquisition workflows used to acquire dynamic $[^{11}\text{C}]\text{DASB}$ data. The workflow consists of scanners providing anatomical information, i.e. MRI scanners at various field strengths (Tesla), various PET scanners, duration of the dynamic PET acquisition, frame sequence used to temporally acquire 4D $[^{11}\text{C}]\text{DASB}$ data, injected dose (ranging from approximately 100-740 MBq), and finally the reconstruction methods used to reconstruct the 4D PET sequence. The colors indicate the frequency per step that has been applied in a $[^{11}\text{C}]\text{DASB}$ PET study out of the total 105 studies. Injected dose is filled as white, because it spans a continuous range and is highly subject-specific. The 4D imaging data are the output of the data acquisition workflow and input to the preprocessing workflow.

the average sensitivity (including 16% scatter) was $251 \text{ cps}\cdot\text{MBq}^{-1}\cdot\text{mL}^{-1}$ for the direct planes, whereas the average sensitivity was $351 \text{ cps}\cdot\text{MBq}^{-1}\cdot\text{mL}^{-1}$ for the cross planes. After the study by Houle et al.³ and until 2008, a total of six DASB studies were conducted with the GEMS scanner, all published by the Center for Addiction and Mental Health, Toronto, Canada, including the first $[^{11}\text{C}]\text{DASB}$ study discussing quantification strategies by Ginovart et al.⁵

After the first publication of $[^{11}\text{C}]\text{DASB}$, attention increased substantially around the World, motivating researchers to investigate new hypotheses related to the serotonin transporter. Consequently, resulting in a large number of different scanners used to map $[^{11}\text{C}]\text{DASB}$ binding. Ogawa et al.⁶ from Japan used an Eminence SET-3000GCT/X PET scanner (performance evaluated in 2006⁷) to investigate the effects of Tramadol for pain treatment; this is currently the only published $[^{11}\text{C}]\text{DASB}$ study using this scanner. Another Japanese group⁸ used an SHR12000 tomograph from Hamamatsu Photonics (performance evaluated in 2002⁹) to study the serotonin transporter in Alzheimer's Disease; this is the only $[^{11}\text{C}]\text{DASB}$ study published using this scanner. Both of these scanners operate in 3D-mode, providing an excellent in-plane spatial resolution ranging from approximately 3 mm FWHM in the center of the FOV to 5 mm FWHM at 10 cm off center. This makes them somewhat ideal PET scanners to capture cortical features of the serotonin transporter, as on average, cortex is only 3 mm thick.¹⁰

The National Institute of Radiological Sciences in Chiba Japan, published two $[^{11}\text{C}]\text{DASB}$ studies in

2006¹¹ and 2010¹²; these were the only studies using an ECAT47 PET scanner. This PET scanner also operates in 3D-mode, but unlike the Eminence and Hamamatsu scanners, which have an axial resolution of 3–5 mm FWHM, this scanner has an in-plane axial spatial resolution of 6.2 mm in the center of the FOV, and 7.2 mm at 10 cm off center.¹³ This means that the spatial resolution is almost half as good in the center of the FOV, and more severe partial volume effects (PVEs) are to be expected. Several integrated PET/CT systems have also been used to map the serotonin transporter, including the Biograph HiRez¹⁴ and the Biograph TruePoint,¹⁵ both manufactured by Siemens, having a spatial resolution of approximately 4.5 mm. A total of seven published $[^{11}\text{C}]\text{DASB}$ PET papers have used this scanner. The most commonly used PET scanners for measuring $[^{11}\text{C}]\text{DASB}$ are the ECAT EXACT HR + PET scanner from Siemens (performance evaluated in 1997¹⁶), the GE Advance PET scanner from General Electric (performance evaluated in 2002¹⁷) and the High Resolution Research Tomography (HRRT) PET scanner from Siemens (performance evaluated in 2002¹⁸). Van Velden et al.¹⁹ directly compared the performances of the HRRT and HR + scanner in 2009. The in-plane spatial resolution of the HRRT is 2.3–3.4 mm FWHM, whereas the in-plane spatial resolution of the HR + scanner is 4.3–8.3 mm FWHM.

Furthermore, the sensitivity of the HRRT is higher than that of the HR + scanner, $39.8 \text{ kcps}\cdot\text{kBq}^{-1}\cdot\text{mL}^{-1}$ compared to $21.9 \text{ kcps}\cdot\text{kBq}^{-1}\cdot\text{mL}^{-1}$, respectively.

Finally, the GE advance PET scanner from General Electric has an in-plane spatial resolution of 4.4 mm

FWHM in the center of the FOV, and 6 mm FWHM in the outer FOV.¹⁷ The GE Advance scanner sensitivity is approximately $27.6 \text{ kcps} \cdot \text{kBq}^{-1} \cdot \text{mL}^{-1}$, placing it as the second best performing scanner regarding scanner sensitivity, with the HRRT in first place, and the ECAT EXACT HR+ in third place.

Our analysis of the reported values from the papers revealed that BP_{ND} in both striatum and ACC was associated with the PET-scanner used in the study. This was also true for the between-subject standard deviation of BP_{ND} (Figure S1). A higher scanner resolution was associated with higher BP_{ND} 's and higher between-subject standard deviations ($P=0.027$).

This means that more subjects are needed to detect a statistical difference in a group analysis.

On the other hand, the larger between-subject variability may also be caused by increased ability to detect subject-specific binding, as reflected by a higher resolution scanner.

The HRRT scanner has high sensitivity, but is limited by relatively small detector elements which means, that the number of acquired counts is lower than in other scanners, potentially resulting in more noisy data.

Moreover, the spatial resolution differs significantly between scanners with the HR+ being nearly isotropic, whereas the GE Advance has a much better axial resolution than transaxial resolution (non-isotropic voxels). This means that the resolution is dependent on the orientation of the image, resulting in different spill-over effects of the tracer in different directions. This makes it difficult to correct for PVEs, and may consequently interact with subsequent preprocessing steps such as motion correction, co-registration and normalization to a standard space.

Instituting a more standardized policy for the reporting/usage of PET scanner performances should ensure that future readers are better able to effectively evaluate and understand the potential biases and uncertainties of the data. We note that researchers often only report the FWHM in the center of the FOV when publishing papers, creating a limited/biased interpretation if cortical regions are the primary region of interest.

In addition, reviewers should pay special attention to the use of 2D reconstruction over 3D reconstruction, non-isotropic over isotropic resolution, and if any additional smoothing steps are applied to the data (e.g. Strecker et al.²⁰), as these steps significantly degrade the spatial resolution.

Anatomical information from magnetic resonance imaging

Several different techniques have been used to provide the anatomical information needed to guide the functional information provided by the PET data. The most common procedure is to acquire an anatomical

T1-weighted Magnetic Resonance Image (MRI) as a reference image and spatially align the two images (co-registration). However, the field-strength of the MRI scanner will have an impact on the reconstructed MRI image, affecting both the subsequent parcellation of the brain into anatomical subregions and the co-registration to the PET data. Tradeoffs between spatial and temporal resolution and signal/noise also matter, but this topic is considered beyond the scope of this paper.

In the reported [¹¹C]DASB studies, the field-strength used for the MRI scanners includes 0.3T,⁸ 0.5T,²¹ 1.5T,²² 3.0T²³ to 7.0T.²⁴ When no MRI is acquired, the PET image is most often either normalized to a common atlas space (e.g. Lanzenberger et al.²⁵), in which generic regions have been predefined, or manual delineations are applied directly on the PET image. This requires additional smoothing or resampling steps and interacts with nearly all data acquisition steps such as the resolution of the PET scanner, duration, framing and injected dose (Figure 2, described in detail below). In addition, because a standard MRI atlas does not follow the subject-specific anatomy (i.e. cortical folding patterns), it is likely that this procedure will exacerbate the PVE when evaluating regional PET distributions compared to when a subject-specific MRI is available.

For example, if the PET-MRI co-registration is inaccurate, the PET signal might seem to originate from white-matter signal instead of gray matter (GM), or vice versa. In total, we found six different methods whereby anatomical information has been extracted. In our analysis, we found no evidence for an impact of choice of MRI-scanner on BP_{ND} or between-subject variation.

The two to date most widely published methods are acquisitions of either a 1.5T (43%) or 3.0T (32%) T1-weighted MRI (Figure 2). Not unexpectedly, the more recent publications tend to use 3T MRI scanners because most institutes regularly update their MR scanners, with newer ones having higher field strength. However, the extent to which differences in MRI acquisition might affect the final outcome of a complex workflow is largely unknown.

Data acquisition (duration, framing, injected dose, reconstruction)

Variations in [¹¹C]DASB PET data acquisition are distributed across a parameter space containing the (1) time duration of the scanning session, (2) dynamic framing (time-sequence), (3) injected dose and (4) PET reconstruction. Unless list mode acquisitions are available, dynamic PET studies are mostly acquired for a fixed time duration, with multiple 3D-frame

acquisitions distributed over a pre-defined time period. However, the chosen framing varies substantially from study to study, and a total of 17 different sequences have been used so far, i.e. framing $\in \{17, 18, 19, 20, 21, 22, 23, 24, 26, 27, 28, 30, 33, 35, 36, 38, 50\}$ frames. This choice will affect the signal distribution within the acquisition space (FOV), since reduced frame length will result in a reduction in true counts per frame, especially in late frames where the radioactive tracer has decayed due to the half-life of ^{11}C (i.e. $\lambda_{1/2} = 20.3$ min). We identified a positive association between number of frames and striatal BP_{ND} and ACC BP_{ND} but closer inspection revealed that this observation was driven mainly by the HRRT-scanner settings from Denmark using 36 frames and the high-resolution SHR12000-scanner from Japan using 38 frames. As high-resolution scanners increase the binding, this effect may be at least partially explained as a scanner \times frames interaction.

The scan duration of these dynamic PET studies also varies substantially, ranging from 30 min to 120 min, i.e. duration $\in \{30, 60, 80, 90, 95, 100, 110, 120\}$ minutes. Although, Ogden et al.²⁶ argued that 100 mins of scanning time was sufficient, this recommendation has not been followed in all subsequent studies, with most studies choosing 90 min of acquisition time (Figure 2). The required duration of scanning time, however, depends on the neuroscientific question, as various brain structures will have different uptake dynamics.²⁷

The injected dose also varies substantially between approximately 100 MBq to 740 MBq, and the dose varies substantially not only between studies, but also between subjects (Table S1).

All studies reported high molar radioactivity; however, it has never been formally established in a test-retest study with substantially different doses, if a higher injected mass (or mass/kg body weight) leads to a reduction in cerebral [^{11}C]DASB binding. In a large sample of 108 individuals from our own group, we found no evidence for an association between global [^{11}C]DASB binding and injected mass/kg (McMahon et al. 2017, unpublished work). In our analysis, we found no evidence for an impact of injected dose on BP_{ND} or between-subject variability.

Depending on the scanner sensitivity, the injected dose can impact signal-to-noise ratio (SNR). Information about, e.g., range of average counts per minute per study/subject could be interesting information to have access to for analysis, as we did not have access to the individual injected doses, but rather the within-study average injected doses.

The reconstruction of the PET images from the scanner has also been differently performed. Morimoto et al.²⁸ compared [^{11}C]DASB binding in seven healthy subjects using images reconstructed

with either a filtered backprojection (FBP) algorithm or the ordered subsets expectation maximization (OSEM) algorithm.

The study by Morimoto et al. was executed using the data acquisition workflow parameters: ECAT EXACT HR+, 1.5T MRI, 90-min dynamic PET acquisition in 2D-mode, 27 frames, injected dose of 170.2 ± 56.1 MBq. While there have been several reports suggesting a small bias using some versions of OSEM,^{29,30} Morimoto et al. reported no statistically significant differences in any regions between images reconstructed with FBP and OSEM, suggesting that these two algorithms may be used interchangeably in the reconstruction of 4D PET data. Certain PET scanners (e.g. the HRRT) do not allow for a direct use of FBP due to the inherent geometry of the scanner, thereby restricting image reconstruction to the use of iterative reconstruction techniques such as the OSEM algorithm. However, techniques have been developed that allow 3D-FBP on the HRRT, but due to poor noise performance they are not widely used. To summarize the data acquisition workflow section, the most widely published workflow consists of: 1.5T MRI (43%), ECAT EXACT HR+ (43%), 90-min acquisition (65%), 26 frames (17%), and FBP to reconstruct the 4D PET data (72%).

The “preprocessing pipeline” for [^{11}C]DASB PET quantification

Motion correction

Motion correction (MC) algorithms for dynamic PET studies have been developed to remove inherent motion artefacts from the data. The most popular head MC technique is between-frame-correction where either all or a subset of the remaining images are registered to a chosen reference image. Of the 105 studies, 43 studies (41%) leave out any type of MC, arguing that fixing the subject in the scanner using, e.g., a thermoplastic mask sufficiently limits motion. Twenty-nine studies used between-frame-correction to correct for motion without explicitly specifying the exact procedure (e.g. James et al.³¹). Twenty-one studies used between-frame-correction to correct for motion, by aligning all frames to a frame with high SNR (e.g. Frokjaer et al.³²). Ten studies used either a mean or a summed PET image over all frames to correct for motion (e.g. Cannon et al. 2007³³), and two studies used either a partially summed image³⁴ or a reference frame³⁵ to perform between-frame MC, but only frames where the researcher observed motion are aligned, leaving the frames without motion untouched.

The latter method not only introduces a user-dependent bias, it also raises the question: given that

motion is present in the data, how much movement is needed in order to perform MC?

Overall, this results in five different ways in which MC has been applied/not applied in the [^{11}C]DASB literature. In our analysis, we grouped the analysis into motion versus no motion and observed a trend for significance ($P=0.064$) of the use of MC and striatal between-subject variability, suggesting that MC lowers between-subject variability in the striatum with 0.035 compared to without MC (Figure S2). This translates into 26% fewer subjects needed in a group analysis to obtain similarly powered statistical tests (see calculation in supplementary).

MC in the absence of motion will lead to some degree of smoothing, which may to some extent account for the observed reduced between-subject variability. In addition, potential effects of motion within a frame are often neglected, even though several solutions have been suggested such as MOLAR⁷⁵ (Motion-Compensation OSEM List-mode Algorithm for Resolution-Recovery Reconstruction) or Tracoline⁷⁶ (List-mode PET MC using markerless head tracking), given that list-mode data are available.

MC is often carried out using different software packages (AIR, FSL and SPM), which all have different implementation and precision of similar methods but based on different cost functions. To our knowledge, the effect of various software packages on MC performance has not yet been investigated in dynamic 4D PET imaging. In addition, frame-by-frame MC without re-doing the image reconstruction may result in errors in attenuation correction, which is often neglected (Van den Heuvel et al.⁷³).

Co-registration

Accurate co-registration of PET and MR images is an important step, not the least when PET Partial Volume Correction (PVC) and parcellation of regions are carried out, when integrating multimodal neuroimaging data.³⁶ Ninety-eight percent of all studies used a normalized mutual information (NMI) registration algorithm to perform the co-registration but the explicit procedure differs across studies that use various software packages, including FSL and SPM. Each co-registration technique is based on a cost-function, aiming to minimize the registration error (e.g. sum of least-squares or mutual information) of the two datasets being aligned (MRI and PET). This cost-function is often based on shared information between the two datasets being aligned (e.g. cortical boundaries), making them somewhat dependent on the intensity distribution and resolution of the acquired data. The remaining 2%^{37,38} used a boundary-based registration (BBR) algorithm to co-register the T1-weighted MRI

with the PET image. BBR also contains a mutual information component, but puts an additional cost on the cortical boundaries being aligned. The co-registration preprocessing step potentially depends on the spatial- and temporal distribution of the PET signal, and will therefore be sensitive to the chosen cost-function. For example, the serotonin transporter is only modestly expressed in the neocortex, and the boundary-based algorithm may therefore not be the optimal registration algorithm to capture cortical folding patterns, particularly not if the PET scanner resolution is limited. In addition, brain areas located in close vicinity to ventricles and cerebrospinal fluid (CSF) will suffer more from PVEs, depending on the resolution of the PET scanner and the radiotracer being used, especially when data with non-isotropic spatial resolution were acquired.

Delineation of volumes of interest

Many neuroimaging experiments are based on hypotheses relating to specific anatomical brain regions, often referred to as VOIs. As mentioned previously, for PET, this generally requires co-registration with a structural MRI scan with anatomical labels. However, there is currently no consensus in the [^{11}C]DASB PET community about which atlas generates the best set of VOIs. Whereas a single study used the probabilistic Harvard-Oxford atlas to delineate VOIs,³¹ 14 published papers used PVElab, which is a data-driven anatomical probability-based labeling approach based on MRI templates from 10 healthy volunteers (e.g. Frokjaer et al.³⁹). Nine studies used the Desikan/Killiany atlas (e.g. from FreeSurfer) which involves a data-driven technique, providing the researcher with a subject-specific anatomical labeling, given that they have acquired a subject-specific T1-weighted MRI (e.g. Ganz et al.³⁷). Seven studies used the anatomical automatic labeling (AAL) atlas offered by the SPM software (e.g. Savli et al.⁴⁰). The AAL atlas does not provide unique subject-specific anatomical labeling, but can be used for group analyses, where all subject-specific PET scans have been normalized to AAL standard space. Seven studies used the Hammers atlas, which is a probabilistic brain atlas based on 83 manually delineated regions drawn on MR images of 30 healthy subjects in native space, subsequently spatially normalized to a standard brain from the Montreal Neurological Institute (MNI) (e.g. Hinz et al.⁴¹). Fourteen studies used an atlas-based procedure, without explicitly stating the exact labeling approach, mostly being based on local procedures and study-specific atlases (e.g. Takano et al.⁴²). These atlases are often based on data obtained from a set of young and healthy subjects, in which manually delineated regions have been drawn in

native subject-space prior to spatial normalization to MNI-space. Ten published studies used an “automatic method” to obtain VOIs, stating that the anatomical labeling was unbiased with respect to any user interactions (e.g. Tyrer et al.¹⁴).

Somewhat surprisingly, 38% of all published [¹¹C]DASB studies included in this review, manually define their own VOIs, also in some recent studies.^{43,44}

In our analysis, we found a striatal BP_{ND} × VOI interaction, suggesting that some definitions of volumes produce either higher or lower BP_{ND} compared to others (Figure S3). Since this step may interact with all previous steps, we are cautious to make any firm conclusions based on this.

Hammers atlas and manual delineations contributed to the most variation, but should ideally also be split into additional sub-categories depending on the operational criteria, and whether the delineation was performed in PET or MRI space (Table S1). In addition, it is expected that the variability will increase as the size of the VOI decreases, but with limited reports on size of VOIs in the published studies, this reduces our ability to assess the impact of atlas choice. Nevertheless, what we can conclude is that the choice of atlas can produce widely different outcomes, as highlighted in Table S1.

Even though manual anatomical labeling seems to be the most popular, it may impose an interrater variability/bias in the subsequent data analysis and interpretation, unless well-defined operational criteria and blindness to subject diagnosis are applied.

Another potential issue with both manual delineation and atlases is that even though the tracer distribution within an anatomical VOI is assumed to be homogeneous, this is often not the case and accordingly, structural homogeneously defined VOIs may therefore misrepresent the radioligand concentration within that region (e.g. the thalamus). Correct anatomical labeling is critically important in many dynamic PET studies, because the PET data suffers significantly from PVEs.

We recommend that researchers provide explicit specifications about VOI definitions in the supplementary material, and if possible, attach the 3D anatomical labelings in appropriate formats. This is an approach also supported by researchers in the fMRI field.⁴⁵

Partial volume correction

In PET studies, it can be difficult to assess the extent to which an observed difference in PET signal is caused by a change in the imaging target distribution, if it is due to less GM, or if it is due to limited PET scanner resolution causing the PET signal to spill in or out of relatively homogeneous tissue regions. Partial Volume Correction (PVC) is not commonly used in

[¹¹C]DASB PET imaging (Figure 3). Only four published [¹¹C]DASB studies have used Muller-Gartner PVC, to correct for PVEs.^{46–48,74}

If there is little evidence for differences in brain volumes, the application of PVC techniques may lead to noise amplification, and extreme care should therefore be taken when interpreting the results.³⁶ In addition, PVC is MR scanner and sequence dependent due to variability of segmentation results from the MRI. For an in-depth discussion of PVC techniques in PET imaging, we refer the reader to the paper by Erlandsson et al.⁴⁹

Quantification of [¹¹C]DASB PET data

The final step in processing of [¹¹C]DASB PET data is kinetic modeling which is applied to the preprocessed 4D PET data. All the kinetic modeling approaches used for quantification of [¹¹C]DASB PET data are displayed in Figure 3, including the frequency of their use. The quantification of tracer kinetics of the serotonin transporter *in vivo* has been applied extensively and in various formats, providing information about binding in specific VOIs. The gold standard is to obtain arterial blood samples in parallel with the dynamic PET scan, providing an arterial input function (AIF) for subsequent kinetic modeling.⁵

However, the use of arterial sampling requires invasive techniques, which often imposes additional discomfort to the subject being scanned. Furthermore, blood sample analysis (on-line vs. manual sampling, including frequency of sampling), metabolite estimation (HPLC or fraction-collector) and interpolation (fitting a power function) can add additional variation to the data analysis. Two-tissue compartment modeling (2TCM) with an AIF is considered state-of-the-art in the PET literature, but once validated, tissue reference methods may be used instead. The kinetic models used in [¹¹C]DASB neuroimaging include both reference tissue methods and methods with an AIF (Figure 3). Reference tissue methods obviate invasive arterial sampling, but they rely on the assumption and identification of a reference region with non-specific binding characteristics.

In the [¹¹C]DASB literature, cerebellum (possibly excluding vermis) serves as a reference region, because it is considered to be devoid of serotonin transporters. However, there is currently no consensus among researchers about the validity of cerebellum as a reference region. Some researchers argue for^{5,40,50} and others against, as DASB binding in the cerebellum has been shown to be displaced by SSRIs.^{51–53} Even among the researchers using cerebellum as a reference region, there is no consensus about how exactly the reference region must be defined.^{37,52,54} A recent

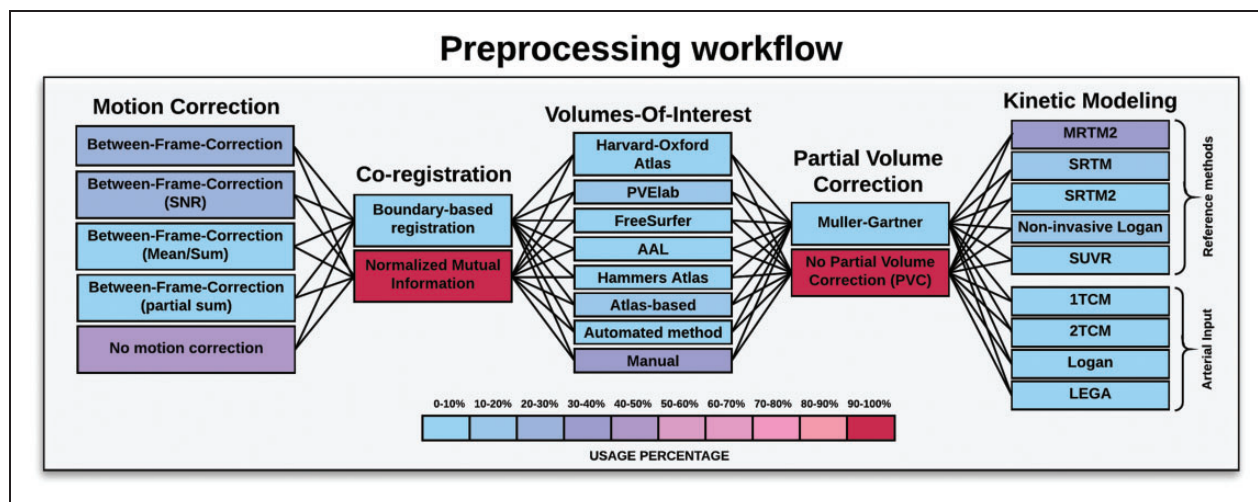


Figure 3. Schematic overview of the various preprocessing steps used in analyzing dynamic [^{11}C]DASB data. This ranges from different motion correction techniques, co-registration, volume-of-interest definitions, partial volume correction, and kinetic modeling. The colors indicate the percentage, in which a given step has been applied in the 105 [^{11}C]DASB PET studies.

investigation of cerebellar heterogeneity and its impact on PET data quantification of 5-HT receptor radioligands, based on a large sample of 100 [^{11}C]DASB HRRT scans, concluded that there are differences in radioactivity uptake between cerebellar subregions.³⁷

New kinetic models are continually being developed and refined, and to date nine different approaches have been applied. Published studies that include blood sampling and use of an AIF over the last couple of years have become less common, with currently four different approaches used to perform the kinetic modeling of [^{11}C]DASB. Only three published studies have used a one-tissue compartment model (1TCM) with an AIF to capture the features of the serotonin transporter.^{5,55,56} Eight studies used a 2TCM with an AIF (e.g. van de Giessen et al.⁵⁷), and eight studies have used the Logan method with an AIF (e.g. Murthy et al.⁵⁸). Finally, the likelihood estimation graphical analysis (LEGA) method (maximum likelihood estimation of the Logan) using an AIF has been used in eight published studies, including one of the three test-retest studies that evaluate reproducibility of [^{11}C]DASB,²⁶ as discussed in more detail below.

Forty-four published studies (38% in total) have used the multilinear reference tissue model 2 (MRTM2), developed by Ichise et al.,⁵⁹ to quantify tracer kinetics of [^{11}C]DASB (e.g. Fisher et al.⁶⁰). Twelve studies used the simplified reference tissue model (SRTM) developed by Lammertsma and Hume in 1996,⁶¹ and eight studies a constrained version of the same model, SRTM2.⁶²

The non-invasive Logan method is used in 22 published studies.⁶³ Finally, four studies have used the ratio of standardized uptake values (SUVR) defined by the

SUV of a given VOI to the SUV of a reference VOI (i.e., the cerebellum has been used as a reference for DASB binding). When using SUVR as a direct measure for binding, the arterial input concentration is assumed to have a consistent shape between studies/subjects, and the area under the arterial input curve is assumed to be proportional to the injected dose/kg body weight.⁶⁴ This assumption applies to all reference techniques, but may be violated as a function of age and/or disease. In terms of equilibrium, one should be careful when selecting the time frame of interest, as this should coincide with the transient equilibrium of the tracer in all subjects.

The SUVR also depends on the rate of peripheral clearance of the tracer; unlike parameters derived from most kinetic models of brain uptake and binding, SUVR is not purely a function of brain parameters, though the extent to which differences in clearance between subjects affects study results has not been carefully examined for [^{11}C]DASB.

Studies that have used SUVR include Lee et al.,⁶⁵ Hesse et al.,⁶⁶ Ginovart et al.⁵ and Houle et al.³ To sum up, nine different methods have been applied to quantify [^{11}C]DASB PET. In our analysis, we find that the choice of kinetic model was associated with between-subject variability of ACC BP_{ND} . SRTM and non-invasive Logan (with Muller-Gartner PVC) produced the highest between-subject variabilities (Figure S4). When adding BP_{ND} as a covariate in the analysis, we also found a trend for a positive association ($P=0.11$) between variation and BP_{ND} , highlighting a potential bias-variance trade-off in ACC BP_{ND} (Figure S5).

The identified bias-variance trade-off as a function of neuroimaging workflow warrants further investigation.

Test–retest studies for [¹¹C]DASB PET

To date, three test–retest studies for [¹¹C]DASB PET imaging have been published.^{26,56,67} These studies involve two different scanners (ECAT HR+ and GE Advance), one fixed time duration (120 min), two different dynamic framings (21 and 33 frames) and a range of 185 MBq to 740 MBq in injected dose. The studies included between 8 to 11 healthy subjects (aged 18–50) with a nearly 50/50 gender distribution. All test–retest scans were performed on the same day.

Two out the three studies used an AIF for the kinetic modeling, whereas one study used MRTM2 with cerebellum as reference region. Ogden et al.²⁶ reported that 100 min of scanning time was sufficient to obtain stable parameter estimates, and that the LEGA kinetic modeling approach produced the best results. However, the LEGA method produced a median percent difference in test–retest binding of approximately 20% ($n=11$, range: 11–39.6%), when taken across all subjects and all VOIs. The median intraclass correlation coefficient (ICC) was approximately $ICC=0.8$ (range: 0.455–0.926), taken across all subjects and all VOIs, with the highest ICC's in the dorsal caudate, thalamus and midbrain. Frankle et al.⁵⁶ obtained slightly higher ICCs compared to Ogden et al.²⁶ with a median ICC of 0.93 ($n=9$, range: 0.79–0.97). Kim et al.⁶⁷ investigating the reproducibility of [¹¹C]DASB binding modeled with MRTM2 ($n=8$), also used ICC as performance metric for test–retest reliability, including the additional performance metrics test–retest bias and test–retest variability. The results showed a significant negative bias in binding across test–retest, and high test–retest reliability for regions such as striatum, thalamus, temporal cortex and occipital cortex ($ICC=0.84$). In contrast, poor test–retest reliability measures were obtained in the raphe and frontal cortex ($ICC=0.445$). The reported negative bias across test–retest was barely discussed by Kim et al. and neither Frankle et al. nor Ogden et al. observed a negative test–retest bias with lower binding at retest.

The overall conclusion by Kim et al. was that the MRTM2 was reproducible and reliable for [¹¹C]DASB studies.

Notably, these test–retest studies were all performed on a relatively small sample and they demonstrate that some methods (i.e. Ogden et al. (LEGA) and Kim et al. (MRTM2)) are better or equally performing compared to other methods. However, the chosen performance metrics are not consistent across test–retest studies, and no attempt is explicitly made to address possible interactions with other preprocessing steps and/or other steps of the workflow (i.e. subject selection and data acquisition), as data acquisition and preprocessing are not consistent across the three test–retest studies. For example, Kim et al. used a summed image to perform frame-based MC, whereas Frankle et al. used a reference

frame. However, while Frankle et al. used VOIs manually determined on MRIs according to well-defined operational criteria in conjunction with automated gray/white/CSF segmentation in cortex, Kim et al. instead used manual delineations without specifying the operational criteria to obtain the VOIs. In addition, even though Frankle et al. and Ogden et al. used the same PET scanner to acquire the data, images were reconstructed into $1.7 \times 1.7 \times 2.4$ mm (non-isotropic) and 2.5×2.5 mm, respectively, with no specification on the z-direction in the latter study. All these modifications from study to study, make it difficult for the reader to infer whether reported methodological improvements are causally related to the new proposed method, or if it is due to a difference in data acquisition and/or preprocessing, limiting the generalizability to other neuroimaging workflows and studies.

Conclusions

In this review, we highlight the remarkable variety of ways in which researchers are currently performing complex neuroimaging studies, while implicitly expecting generalizable results across research groups. We systematically reviewed 105 published [¹¹C]DASB studies from 21 different PET centres, outlining differences in subject selection, data acquisition and preprocessing. Data sharing initiatives may significantly contribute to the understanding of the generalizable impact on such complex workflows, as the combined effects resulting from subject selection, data acquisition and preprocessing are unclear. We still need to understand the importance of bias-variance tradeoffs in neuroimaging experiments, and how neuroimaging workflows can be optimized for particular neuroscientific questions. The purpose of this study was not to identify a definitive PET preprocessing pipeline, but rather to establish workflow-dependent effects on binding and variation.

It is to be expected that the application of a new preprocessing pipeline will lead to different absolute binding measures, but the important question is whether the outcome of a study (i.e. difference between patients and controls) will remain.

In order to evaluate the extent to which any of the methodological factors described in this review matters, one needs to consider the given study aims.

For example, if an investigator wishes to compare age effects on the serotonin transporter in the striatum between two studies, it might be tempting to use both data sets, given that the methodology is internally consistent. However, while the researcher may not be able to combine the two sets of data, he/she may be able to use the two data sets separately, assuming that the derived parameters while different, are scalable. For future data sharing initiatives, it would be

beneficial in a large and complete data set across a large number of subjects to assess which differences the various methodological variations can lead to, e.g. how much of a difference does variation in scanner resolution impact on, e.g., the striatum.

Our review focused on the radioligand [^{11}C]DASB, but the same considerations underlying the [^{11}C]DASB workflows could be made for any given PET or SPECT radiotracer. The aim of our paper is to highlight the need for transparency, reproducibility and to support future data sharing opportunities in the PET neuroimaging community. It is our hope that this work can also be used as a tool for future studies to evaluate the extent to which a given study deviates significantly from the current literature. From the current literature, it can be difficult to infer whether an observed change is physiological, or if it is driven by changes in subject selection and/or data acquisition and/or preprocessing. Data acquisition and preprocessing pipelines and their experimental interactions seem to be an overlooked aspect in modern PET neuroscience, and we believe that such testing is necessary in order to reliably provide new insights into human brain function.

Funding

The author(s) disclosed receipt of the following financial support for the research, authorship, and/or publication of this article: MN was supported by the National Institutes of Health (Grant 5R21EB018964-02), the Lundbeck Foundation (Grant R90-A7722), and the Independent Research Fund Denmark (DFE-1331-00109 & DFF-4183-00627).

Declaration of conflicting interests

The author(s) declared no potential conflicts of interest with respect to the research, authorship, and/or publication of this article.

Supplementary material

Supplementary material for this paper can be found at the journal website: <http://journals.sagepub.com/home/jcb>

References

- Wilson AA, Ginovart N, Schmidt ME, et al. Novel radiotracers for imaging the serotonin transporter by positron emission tomography: synthesis, radiosynthesis, in vitro, and ex vivo evaluation of [^{11}C]-labelled 2-(phenylthio)araalkylamines. *J Med Chem* 2000; 43: 3103–3110.
- Rylands AJ, Hinz R, Jones M, et al. Pre- and postsynaptic serotonergic differences in males with extreme levels of impulsive aggression without callous unemotional traits: a PET study using ^{11}C -DASB and ^{11}C -MDL100907. *Biolog Psychiatry* 2012; 72: 1004–1011.
- Houle S, Ginovart N, Hussey D, et al. Imaging the serotonin transporter with positron emission tomography: initial human studies with [^{11}C]DAPP and [^{11}C]DASB. *Eur J Nucl Med* 2000; 27: 1719–1722.
- Holte S, Eriksson L and Dahlbom M. A preliminary evaluation of the Scanditronix PC1048-15B brain scanner. *Eur J Nucl Med* 1989; 15: 719–721.
- Ginovart N, Wilson AA, Meyer JH, et al. Positron emission tomography quantification of [^{11}C]DASB binding to the human serotonin transporter: modeling strategies. *J Cereb Blood Flow Metab* 2001; 21: 1342–1353.
- Ogawa K, Tateno A, Arakawa R, et al. Occupancy of serotonin transporter by tramadol: a positron emission tomography study with [^{11}C]DASB. *Int J Neuropsychopharmacol* 2014; 17: 845–850.
- Matsumoto K, Kitamura K, Mizuta T, et al. Performance characteristics of a new 3-dimensional continuous emission and spiral-transmission high sensitivity and high-resolution PET camera evaluated with the NEMA NU 2-2001 standard. *J Nucl Med* 2006; 47: 83–90.
- Ouchi Y, Yoshikawa E, Futatsubashi M, et al. Altered brain serotonin transporter and associated glucose metabolism in Alzheimer disease. *J Nucl Med* 2009; 50: 1260–1266.
- Watanabe M, Shimizu K, Omura T, et al. A new high-resolution PET scanner dedicated to brain research. *IEEE Trans Nucl Sci* 2002; 49: 634–639.
- Fischl B and Dale AM. Measuring the thickness of the human cerebral cortex from magnetic resonance images. *Proc Natl Acad Sci U S A* 2000; 97: 11050–11055.
- Takano A, Suzuki K, Kosaka J, et al. A dose-finding study of duloxetine based on serotonin transporter occupancy. *Psychopharmacology* 2006; 185: 395–399.
- Matsumoto R, Ichise M, Ito H, et al. Reduced serotonin transporter binding in the insular cortex in patients with obsessive-compulsive disorder: a [^{11}C]DASB PET study. *Neuroimage* 2010; 49: 121–126.
- Kim JS, Lee JS, Lee DS, et al. Performance evaluation of Siemens CTI ECAT EXACT 47 PET scanner using NEMA NU2-2001. *IEEE Nucl Sci Symp Conf Record* 2004; 5: 3118–3120.
- Tyrer AE, Levitan RD, Houle S, et al. Serotonin transporter binding is reduced in seasonal affective disorder following light therapy. *Acta Psychiatr Scand* 2016; 134: 410–419.
- Kim E, Howes OD, Park JW, et al. Altered serotonin transporter binding potential in patients with obsessive-compulsive disorder under escitalopram treatment: [^{11}C]DASB PET study. *Psychol Med* 2016; 46: 357–366.
- Adam L-E, Zaers J, Ostertag H, et al. Performance evaluation of the whole-body PET scanner ECAT EXACT HR/sup +/- following the IEC standard. *IEEE Transac Nucl Sci* 1997; 44: 1172–1179.
- Khohlmyer S and Stearns C. NEMA NU2-2001 performance results for the GE Advance PET system. *IEEE Record* 2002; 100: 890–894.
- Wienhard K, et al. The ECAT HRRT: performance and first clinical application of the new high resolution research tomograph. *IEEE Trans Nucl Sci* 2002; 49: 104–110.
- van Velden FH, Kloet RW, van Berckel BN, et al. HRRT versus HR + human brain PET studies: an interscanner test-retest study. *J Nucl Med* 2009; 50: 693–702.

20. Strecker K, Wegner F, Hesse S, et al. Preserved serotonin transporter binding in de novo Parkinson's disease: negative correlation with the dopamine transporter. *J Neurol* 2011; 258: 19–26.
21. Bhagwagar Z, Murthy N, Selvaraj S, et al. 5-HTT binding in recovered depressed patients and healthy volunteers: a positron emission tomography study with [¹¹C]DASB. *Am J Psychiatr* 2007; 164: 1858–1865.
22. Politis M, Wu K, Loane C, et al. Serotonergic mechanisms responsible for levodopa-induced dyskinesias in Parkinson's disease patients. *J Clin Invest* 2014; 124: 1–10.
23. Lee JY, Seo S, Lee JS, et al. Putaminal serotonergic innervation. *Neurology* 2015; 85: 853–860.
24. Kim JH, Son YD, Kim JH, et al. Serotonin transporter availability in thalamic subregions in schizophrenia: a study using 7.0-T MRI with [¹¹C]DASB high-resolution PET. *Psychiatry Res* 2015; 231: 50–57.
25. Lanzenberger R, Kranz GS, Haeusler D, et al. Prediction of SSRI treatment response in major depression based on serotonin transporter interplay between median raphe nucleus and projection areas. *Neuroimage* 2012; 63: 874–881.
26. Ogden RT, Ojha A, Erlandsson K, et al. In vivo quantification of serotonin transporters using [¹¹C]DASB and positron emission tomography in humans: modeling considerations. *J Cereb Blood Flow Metab* 2007; 27: 205–217.
27. Frankle WG, Huang Y, Hwang DR, et al. Comparative evaluation of serotonin transporter radioligands ¹¹C-DASB and ¹¹C-McN 5652 in healthy humans. *J Nucl Med* 2004; 45: 682–694.
28. Morimoto T, Ito H, Takano A, et al. Effects of image reconstruction algorithm on neurotransmission PET studies in humans: comparison between filtered backprojection and ordered subsets expectation maximization. *Ann Nucl Med* 2006; 20: 237–243.
29. Bélanger MJ, Mann JJ and Parsey RV. OS-EM and FBP reconstructions at low count rates: effect on 3D PET studies of [¹¹C] WAY-100635. *Neuroimage* 2004; 21: 244–250.
30. Boellaard R, van Lingen A and Lammertsma AA. Experimental and clinical evaluation of iterative reconstruction (OSEM) in dynamic PET: quantitative characteristics and effects on kinetic modeling. *J Nucl Med* 2001; 42: 808–817.
31. James GM, Baldinger-Melich P, Philippe C, et al. Effects of selective serotonin reuptake inhibitors on interregional relation of serotonin transporter availability in major depression. *Front Hum Neurosci* 2017; 11: 48.
32. Frokjaer VG, Pinborg A, Holst KK, et al. Role of serotonin transporter changes in depressive responses to sex-steroid hormone manipulation: a positron emission tomography study. *Biol Psychiatr* 2015; 78: 534–543.
33. Cannon DM, et al. Elevated serotonin transporter binding in major depressive disorder assessed using positron emission tomography and [¹¹C]DASB: comparison with bipolar disorder. *Biol Psychiatr* 2007; 62: 870–877.
34. Vanicek T, Kutzelnigg A, Philippe C, et al. Altered interregional molecular associations of the serotonin transporter in attention deficit/hyperactivity disorder assessed with PET. *Hum Brain Mapp* 2017; 38: 792–802.
35. Politis M, Wu K, Loane C, et al. Serotonin neuron loss and nonmotor symptoms continue in Parkinson's patients treated with dopamine grafts. *Sci Transl Med* 2012; 4: 128ra41.
36. Greve DN, Salat DH, Bowen SL, et al. Different partial volume correction methods lead to different conclusions: an ¹⁸F-FDG-PET study of aging. *Neuroimage* 2016; 132: 334–343.
37. Ganz M, Feng L, Hansen HD, et al. Cerebellar heterogeneity and its impact on PET data quantification of 5-HT receptor radioligands. *J Cereb Blood Flow Metab* 2017; 37: 3243–3252.
38. Beliveau V, Svarer C, Frokjaer VG, et al. Functional connectivity of the dorsal and median raphe nuclei at rest. *Neuroimage* 2015; 116: 187–195.
39. Frokjaer VG, Vinberg M, Erritzoe D, et al. High familial risk for mood disorder is associated with low dorsolateral prefrontal cortex serotonin transporter binding. *Neuroimage* 2009; 46: 360–366.
40. Savli M, Bauer A, Mitterhauser M, et al. Normative database of the serotonergic system in healthy subjects using multi-tracer PET. *Neuroimage* 2012; 63: 447–459.
41. Hinz R, Selvaraj S, Murthy NV, et al. Effects of citalopram infusion on the serotonin transporter binding of [¹¹C]DASB in healthy controls. *J Cereb Blood Flow Metab* 2008; 28: 1478–1490.
42. Takano A, Suzuki K, Kosaka J, et al. A dose-finding study of duloxetine based on serotonin transporter occupancy. *Psychopharmacology* 2006; 185: 395–399.
43. Zientek F, Winter K, Müller A, et al. Effortful control as a dimension of temperament is negatively associated with prefrontal serotonin transporter availability in obese and non-obese individuals. *Eur J Neurosci* 2016; 44: 2460–2424.
44. Roussakis AA, Politis M, Towey D, et al. Serotonin-to-dopamine transporter ratios in Parkinson disease. *Neurology* 2016; 86: 1152–1158.
45. Poldrack RA, Fletcher PC, Henson RN, et al. Guidelines for reporting an fMRI study. *Neuroimage* 2008; 40: 409–414.
46. Frokjaer VG, Erritzoe D, Holst KK, et al. Prefrontal serotonin transporter availability is positively associated with the cortisol awakening response. *Eur Neuropsychopharmacol* 2013; 23: 285–294.
47. Frokjaer VG, Erritzoe D, Holst KK, et al. In abstinent MDMA users the cortisol awakening response is off-set but associated with prefrontal serotonin transporter binding as in non-users. *Int J Neuropsychopharmacol* 2014; 17: 1119–1128.
48. Marner L, Frokjaer VG, Kalbitzer J, et al. Loss of serotonin 2A receptors exceeds loss of serotonergic projections in early Alzheimer's disease: a combined [¹¹C]DASB and [¹⁸F]altanserin-PET study. *Neurobiol Aging* 2012; 33: 479–487.
49. Erlandsson K, Buvat I, Pretorius PH, et al. A review of partial volume correction techniques for emission tomography and their applications in neurology, cardiology and oncology. *Phys Med Biol* 2012; 57: R119–R159.

50. Nogami T, Takano H, Arakawa R, et al. Occupancy of serotonin and norepinephrine transporter by milnacipran in patients with major depressive disorder: a positron emission tomography study with [¹¹C]DASB and (S,S)-[¹⁸F]FMENR-D(2). *Int J Neuropsychopharmacol* 2013; 16: 937–943.
51. Miller JM, Everett BA, Oquendo MA, et al. Positron emission tomography quantification of serotonin transporter binding in medication-free bipolar disorder. *Synapse* 2016; 70: 24–32.
52. Parsey RV, Kent JM, Oquendo MA, et al. Acute occupancy of brain serotonin transporter by sertraline as measured by [¹¹C]DASB and positron emission tomography. *Biol Psychiatr* 2006; 59: 821–828.
53. Shapiro PA, Sloan RP, Deochand C, et al. Quantifying serotonin transporters by PET with [¹¹C]-DASB before and after interferon-alpha treatment. *Synapse* 2014; 68: 548–555.
54. Kish SJ, Furukawa Y, Chang LJ, et al. Regional distribution of serotonin transporter protein in postmortem human brain: is the cerebellum a SERT-free brain region? *Nucl Med Biol* 2005; 32: 123–128.
55. McCann UD, Szabo Z, Seckin E, et al. Quantitative PET studies of the serotonin transporter in MDMA users and controls using [¹¹C]McN5652 and [¹¹C]DASB. *Neuropsychopharmacology* 2005; 30: 1741–1750.
56. Frankle WG, Slifstein M, Gunn RN, et al. Estimation of serotonin transporter parameters with ¹¹C-DASB in healthy humans: reproducibility and comparison of methods. *J Nucl Med* 2006; 47: 815–826.
57. van de Giessen E, Rosell DR, Thompson JL, et al. Serotonin transporter availability in impulsive aggressive personality disordered patients: a PET study with [¹¹C]DASB. *J Psychiatr Res* 2014; 58: 147–154.
58. Murthy NV, Selvaraj S, Cowen, et al. Serotonin transporter polymorphisms (SLC6A4 insertion/deletion and rs25531) do not affect the availability of 5-HTT to [¹¹C]DASB binding in the living human brain. *Neuroimage* 2010; 52: 50–54.
59. Ichise M, Liow J-S, Lu J-Q, et al. Linearized reference tissue parametric imaging methods: application to [¹¹C]DASB positron emission tomography studies of the serotonin transporter in human brain. *J Cereb Blood Flow Metab* 2003; 23: 1096–1112.
60. Fisher PM, Ozenne B, Svarer C, et al. BDNF val66met association with serotonin transporter binding in healthy humans. *Transl Psychiatr* 2017; 7: e1029.
61. Lammertsma AA and Hume SP. Simplified reference tissue model for PET receptor studies. *Neuroimage* 1996; 4: 153–158.
62. Wu Y and Carson RE. Noise reduction in the simplified reference tissue model for neuroreceptor functional imaging. *J Cereb Blood Flow Metab* 2002; 22: 1440–1452.
63. Logan J, Fowler JS, Volkow ND, et al. Distribution volume ratios without blood sampling from graphical analysis of PET data. *J Cereb Blood Flow Metab* 1996; 16: 834–840.
64. Yoder KK, Territo PR, Hutchins GD, et al. Comparison of standardized uptake values with volume of distribution for quantitation of [¹¹C]PBR28 brain uptake. *Nucl Med Biol* 2015; 42: 305–308.
65. Lee JY, Seo S, Lee JS, et al. Putaminal serotonergic innervation. *Neurology* 2015; 85: 853–860.
66. Hesse S, Brust P, Mäding P, et al. Imaging of the brain serotonin transporters (SERT) with ¹⁸F-labelled fluoromethyl- McN5652 and PET in humans. *Eur J Nucl Med Mol Imag* 2012; 39: 1001–1011.
67. Kim JS, Ichise M, Sangare J, et al. PET Imaging of serotonin transporters with [¹¹C]DASB: test-retest reproducibility using a multilinear reference tissue parametric imaging method. *J Nucl Med* 2006; 47: 208–214.
68. Button KS, Ioannidis JPA, Mokrysz C, et al. Power failure: why small sample size undermines the reliability of neuroscience. *Nat Rev Neurosci* 2013; 14: 365–376.
69. Moses-Kolko EL, Price JC, Shah N, et al. Age, sex, and reproductive hormone effects on brain serotonin-1A and serotonin-2A receptor binding in a healthy population. *Neuropsychopharmacology* 2011; 36: 2729–2740.
70. Jovanovic H, Lundberg J, Karlsson P, et al. Sex differences in the serotonin 1A receptor and serotonin transporter binding in the human brain measured by PET. *Neuroimage* 2008; 39: 1408–1419.
71. Liu X, Cannon DM, Akula N, et al. A non-synonymous polymorphism in galactose mutarotase (GALM) is associated with serotonin transporter binding potential in the human thalamus: results of a genome-wide association study. *Mol Psychiatr* 2011; 16: 584–594.
72. Tuominen L, Miettunen J, Cannon DM, et al. Neuroticism associates with cerebral in vivo serotonin transporter binding differently in males and females. *Int J Neuropsychopharmacol* 2017; 20: 963–970.
73. van den Heuvel OA, Boellaard R, Veltman DJ, et al. Attenuation correction of PET activation studies in the presence of task-related motion. *Neuroimage* 2003; 19: 1501–1509.
74. Boileau I, Warsh JJ, Guttman M, et al. Elevated serotonin transporter binding in depressed patients with Parkinson's disease: a preliminary PET study with [¹¹C]DASB. *Mov Disord* 2008; 23: 1776–1780.
75. Carson RE, Barker C, Liow JS, et al. Design of a motion-compensation OSEM List-mode Algorithm for resolution-recovery Reconstruction for the HRRT. *IEEE Nucl Sci Symp Conf Record* 2003; 5: 3281–3285.
76. Olesen OV, Sullivan JM, Mulnix T, et al. List-mode PET motion correction using markerless head tracking: proof-of-concept with scans of human subject. *IEEE Trans Med Imag* 2013; 32: 200–209.